Geomechanics and Engineering, *Vol. 33, No. 1 (2023) 41-51*
https://doi.org/10.12989/gae.2023.33.1.041

Triaxial shear behavior of calcium sulfoaluminate (CSA)-treated sand under high confining pressures

James Innocent Ocheme[a], Sakiru Olarewaju Olagunju[b], Ruslan Khamitov[c], Alfrendo Satyanaga[d], Jong Kim[e] and Sung-Woo Moon[*]

Department of Civil and Environmental Engineering, Nazarbayev University, Nur Sultan, 010000, Kazakhstan

(*Received November 22, 2022, Revised February 27, 2023, Accepted March 3, 2023*)

Abstract. Cementitious materials such as Ordinary Portland Cement (OPC), fly ash, lime, and bitumen have been employed for soil improvement over the years. However, due to the environmental concerns associated with the use of OPC, substituting OPC with calcium sulfoaluminate (CSA) cement offers good potential for ground improvement because it is more eco-friendly. Although earlier research has investigated the stabilizing effects of CSA cement-treated sand, no attempt has been made to examine soil behavior under high confining pressure. As a result, this study aimed to investigate the shear strength and mechanical behavior of CSA cement-treated sand using a consolidated drained (CD) triaxial test with high confining pressure. The microstructure of the examined sand samples was investigated using scanning electron microscopy. This study used sand with CSA cement contents of 3%, 5%, and 7% and confining pressures of 0.5, 1.0, and 1.5 MPa. It revealed that the confining pressures and CSA cement content significantly affected the stress-strain and volumetric change behavior of CSA cement-treated sand at high confining pressures.

Keywords: calcium sulfoaluminate; consolidated drained triaxial test; high pressure; shear strength; volume change

1. Introduction

Soil improvement has been used to enhance the engineering behavior of soil by increasing its stability, compressibility, and bearing capacity. For example, numerous researchers have investigated cementitious materials such as lime, fly ash, biopolymer, plastic waste, and ordinary portland cement (OPC) to develop a more effective soil-stabilizing material (Chang and Cho 2014, Chang *et al.* 2016, Ghiyas and Bagheripour 2020, Kazmi 2020, Mahedi *et al.* 2020, Singh *et al.* 2018). Moreover, several studies have highlighted the need to examine how the degree of cementation affects the strength and mechanical properties of cemented-treated soils (Armaghani *et al.* 2020, Marri *et al.* 2012, Schnaid *et al.* 2001, Ud-din *et al.* 2011). However, despite its durability and strength, OPC is becoming less desirable for construction and geotechnical applications because of its significant carbon emissions. The world mean temperature has been continuously rising, and geotechnical applications account for roughly 7% of carbon dioxide emissions from cement production (Sargent *et al.* 2016).

Given the yearly increase in cement usage and the anticipated production of 3340 million metric tonnes by the end of 2030, there is an urgent need for an environmentally friendly binder that does not compromise the improved soil's engineering properties (Schneider *et al.* 2011). For example, calcium sulfoaluminate (CSA) cement, which has the primary component of ye'elimite, produces a lesser carbon footprint than OPC (Juenger *et al.* 2011). Furthermore, because CSA cement possesses admirable characteristics such as fast strength gain, excellent resistance to freeze-thaw cycles, and resistance to harsh environments, CSA has been examined as one of the options for soil stabilization and improvement (Assel *et al.* 2020, Bazarbekova *et al.* 2021, Bisserik *et al.* 2021, Jumassultan *et al.* 2021, Moon *et al.* 2020, Pooni *et al.* 2020, Sagidullina *et al.* 2022a, b, Subramanian *et al.* 2018, Vinoth *et al.* 2018).

Although few studies on cemented soils have investigated the behavior of soils under low to moderate confining pressures, just a few have examined the impact of high confining pressures (Airey 1993, Amini and Hamidi 2014, Clough *et al.* 1981, Consoli *et al.* 1996, Schnaid *et al.* 2001). Even though most engineering problems occur at low confining pressures, studying soil behavior at high pressure is essential to understand better conditions, such as deep pile foundations, tunnels, high earth dams, and offshore piling (Marri *et al.* 2012). Therefore, this study aims to investigate the shear strength and mechanical behavior of CSA cement-treated sand using a consolidated drained (CD) triaxial test with high confining pressure. Different confining pressures ranging from 0.5 MPa to 1.5 MPa were employed to represent different depths of the deep foundation. The behavior of the cemented sample

*Corresponding author, Assistant Professor
E-mail: sung.moon@nu.edu.kz
[a]Graduate Student
[b]Graduate Student
[c]Undergraduate Student
[d]Assistant Professor
[e]Professor

ISSN: 2005-307X (Print), 2092-6219 (Online)

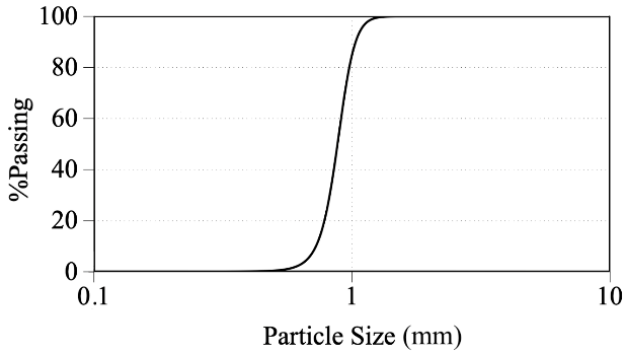

Fig. 1 Quartz sand particle distribution curve used for this research

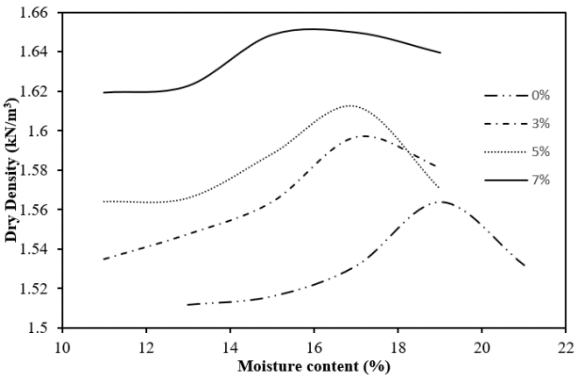

Fig. 2 Compaction curve of CSA-treated soil

Table 1 Quartz sand physical properties

Properties	Value
Effective diameter (D_{10}) (mm)	0.65
Effective diameter (D_{60}) (mm)	0.95
Coefficient of uniformity C_u	1.46
Coefficient of curvature C_c	0.96
USCS	SP
Specific gravity	2.64

Table 2 Standard Proctor Test results for CSA-treated sand

CSA content (%)	Optimum Moisture Content (OMC) (%)	Maximum Dry Density (MDD) (kN/m^3)
0	19.00	1.56
3	17.25	1.59
5	16.75	1.61
7	15.75	1.65

under stress-strain and volumetric change during the CD triaxial test was also discussed.

2. Materials and method

2.1 Materials

In this study, quartz sand, with the Unified Soil Classification System (USCS) classified as "SP" (poorly graded), was used. Table 1 lists the basic properties of the quartz sand. The particle size distribution curve is illustrated in Fig. 1.

Calcium sulfoaluminate (CSA) and gypsum were also used to prepare test samples. The CSA cement primarily contains ye'elimite (C_4A_3S or $4CaO_3Al_2O_3$), belite, and gehlinite. The ye'elimite permits the manufacturing process to be environmentally beneficial, whereas the alite in conventional ordinary Portland cement produces roughly 2.7 times as much carbon dioxide than ye'elimite (Gartner 2004, Jumassultan *et al.* 2021). According to Subramanian *et al*. (2019), (Ukrainczyk *et al.* 2013), the amount of gypsum in a binder has been shown to impact the hydration of CSA cement significantly. Based on the presence of gypsum, the reaction shows the hydration process of ye'elimite (Jumassultan *et al.* 2021). The end product of the hydration process is ettringite, and its chemical formula is $6CaO \cdot Al_2O3 \cdot 3SO3 \cdot 32H_2O$ or $C_3A \cdot 3CS \cdot 32H$.

$$4CaO \cdot 3Al_2O_3 \cdot SO_3 + 2CaSO_4 \cdot 2H_2O + 32H_2O \rightarrow 6CaO \cdot Al_2O_3 \cdot 3SO_3 \cdot 32H_2O + 4Al(OH) \quad (1)$$

Subramanian *et al.* (2019) examined a considerable increase in initial strength and a sustained rise in strength when 30% of CSA cement was substituted with gypsum. Hence, for this study, the optimal gypsum content of 30% was employed to replace a portion of the CSA contents.

2.2 Sample preparation

For sample preparation, the sand was mixed with cement contents of 3%, 5%, and 7% and gypsum, respectively, by the total mass of the dry sand. The CSA cement-sand mixture was mixed for 5 minutes with an automatic mixer until a uniform appearance was achieved. Then, based on the standard proctor test (ASTM/D698, 2012) water was added to the mixture and mixed for 10 minutes. The optimum moisture content (OMC) for sand samples containing 0%, 3%, 5%, and 7% CSA cement are shown in Table 3, which were 19%, 17.25%, 16.75%, and 15.75%, respectively. After mixing, the samples were compacted in three layers in a cylindrical mold with a 38 mm diameter and 76 mm height. The inner walls of the cylindrical steel molds were lubricated with oil to facilitate specimen extrusion. Each of the three layers was compacted 25 times using a rammer. The top of the first and second compaction layers was scarified to avoid problems associated with smooth compaction planes and to provide enough surface-to-surface contact before the placement and compaction of the subsequent layer (Ding *et al.* 2018). After three days, the samples were extruded, wrapped in a plastic membrane to prevent moisture loss, and stored in a humidified room. Due to the rapid increase in strength of CSA-stabilized soils, 7 and 14 days were chosen as the curing period.

2.3 Testing system

The testing was performed by an Environmental Triaxial Automated System (ETAS) manufactured by GDS. Fig. 3 shows the testing system and a photograph of the high-pressure triaxial cell after it was assembled. The system

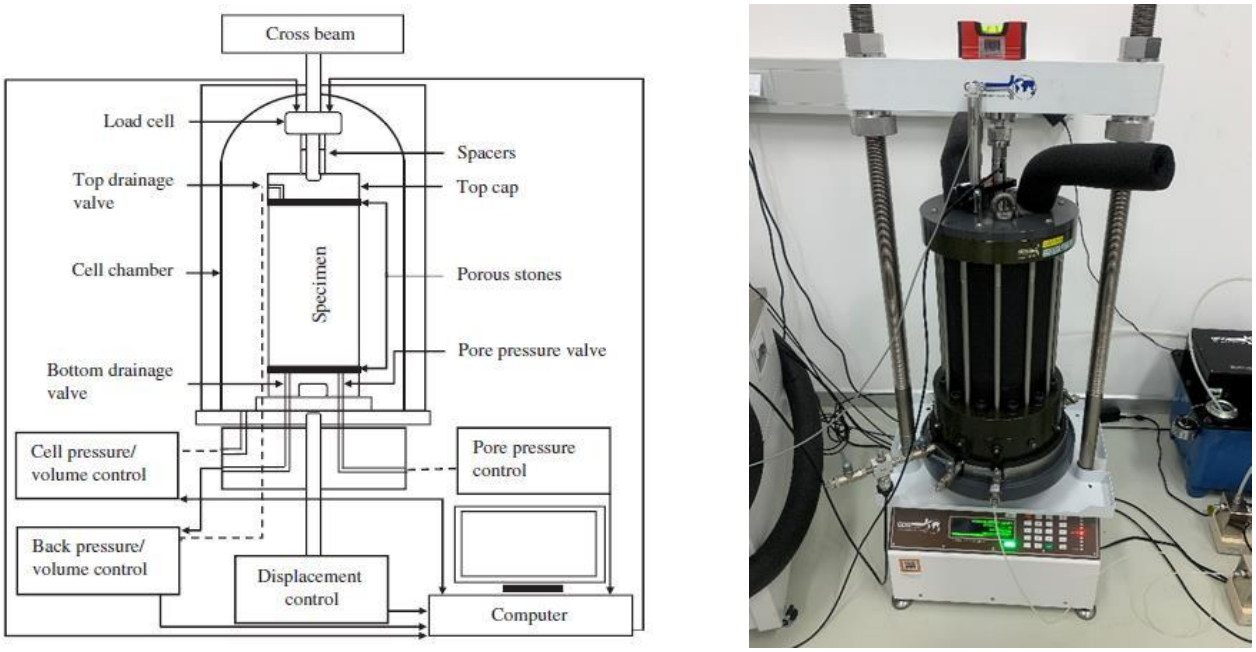

(a) (b)

Fig. 3 GDS Triaxial Automated System: (a) Schematic diagram and (b) Photograph of the high-pressure triaxial cell in the loading frame

components include the triaxial cell, pressure/volume controllers, velocity-controlled load frames, pedestal, top cap, PWP/axial displacement transducer, GDSlab control software, and data logger. The two digital pressure/volume controllers apply and regulate the cell and back pressure during the test. Using a digital hydraulic force actuator, the load was applied to the system from the bottom of a loading frame. The pore water pressure transducer measured the PWP at the sample's base. The cell and back pressure/volume controllers utilized in this study have a pressure capacity of 4 MPa, while the triaxial cell and load cell have a capacity of 4MPa and 50kN, respectively.

2.4 Test procedure

After curing, the test sample was positioned on the top of the base pedestal of the ETAS triaxial cell. The sample was then covered with a rubber membrane to separate it from the pressured chamber oil, and two filter papers and porous stones were placed beneath and on top of it. Two o-rings were fitted around the sample and the base pedestal to prevent cell oil from entering. The high-pressure cell was then assembled and then filled with distilled oil. For saturation, the sample was flushed with de-aired water from top to bottom for two hours, with the back pressure 10kPa lower than the cell pressure. Next, the back and cell pressure were increased simultaneously until Skempton's value was greater than or equal to 0.90 (Lee1a *et al*. 2019, Schnaid *et al.* 2001). After which, it was then consolidated to the required confining pressure at 0.5, 1.0, and 1.5 MPa, respectively, and sheared under drained conditions. The test samples were sheared by applying an axial strain at a constant rate of 0.1mm/min. The consolidated drained (CD) triaxial test was carried out in accordance with ASTM/D7181-20 (2015).

3. Results and analysis

This study conducted consolidated drained (CD) triaxial tests on CSA-treated and untreated sand samples. The samples were consolidated to mean effective stresses of 0.5, 1.0, and 1.5 MPa and shear under a drained condition with σ'_3 remaining constant. The stress-strain and volumetric strain curves for the tested treated sand samples containing 3%, 5%, and 7% CSA cement are shown in Figs. 4 and 5. Figs. 4 and 5 show that the treated sand behavior is highly influenced by the addition of CSA cement and confining pressure. It can be observed that increasing the confining pressures also increases the treated samples' initial stiffness and peak deviator stress. As cement content increases, the peak deviator stress increases, and the peak axial strain decreases. Hence, the treated samples' stress-strain curve changes from ductile to brittle as the CSA cement content increases. It can be seen from the figures that there is a tendency for the stress-strain curves to reach a peak deviator stress followed by subsequent strain-softening for all tested samples for 5% and 7% CSA cement content at the curing periods of 7 and 14 days. For the samples treated with 3% CSA, the stress-strain curves reach a peak deviator stress followed by subsequent strain-softening for 14 days of curing. However, depending on the confining pressure range, it shows a different trend for 7 days of curing as the strain-softening changed into a strain hardening for samples sheared at 1 and 1.5 MPa. Nevertheless, a strain-softening stress-strain behavior was observed for samples treated between 3% CSA under 0.5 MPa and 5% CSA under 1 MPa, and 7% CSA under 1.5 MPa. These differences were due to the degree of cementation, different confining pressure, and the effect of curing days.

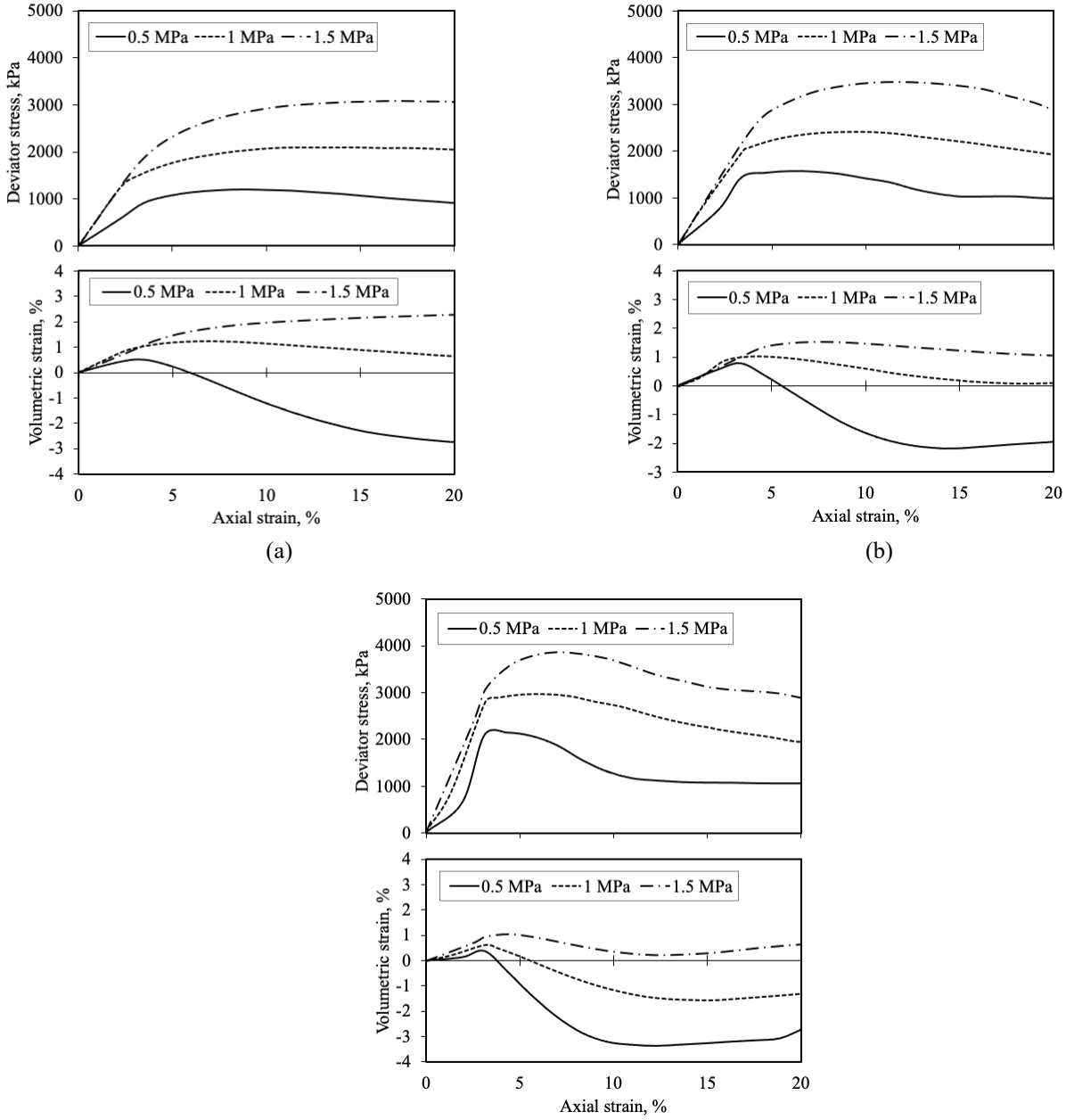

Fig. 4 Stress-strain relationship and volume change behavior of the CSA-treated sand sample: (a) 3%, (b) 5% and (c) 7%, for 7 days of curing

The volumetric strain curves of the tests carried out on the CSA-treated sand samples are also shown in Figs. 4 and 5. A volumetric compression was observed in experiments done for 3% and 5% at σ'_3 = 1.0 MPa and 1.5 MPa, and 1.5 MPa for 7% samples for 7 days of curing. For all of the tests conducted at 0.5 MPa, there was an initial compression followed by a gradual volumetric dilatation.

In addition, an initial volumetric compression was observed, followed by a slow dilatation for samples tested after 14 days of curing, except for 3% and 5% samples sheared at σ'_3 = 1.5 MPa, which exhibited a volumetric compression. Also, it can be observed from the volumetric strain curves that as the cement content increases, the tested samples experience a more dilative behavior during shearing. Hence, with an increase in the cement content, there is a reduction in the compression of CSA-treated samples under various confining pressures. Figs. 4 and 5 also show that the volumetric strain curves attained a constant value toward the end of each test. In light of this, the ultimate state obtained from stress-strain curves might be similar to the critical state for the CSA-treated samples used in this study. In addition, the confining pressure increases the peak deviator stresses, the peak axial strain, and the compression level during shearing. Therefore, with increased confining pressure, the stress-stress behavior becomes ductile. However, the CSA cement concentration

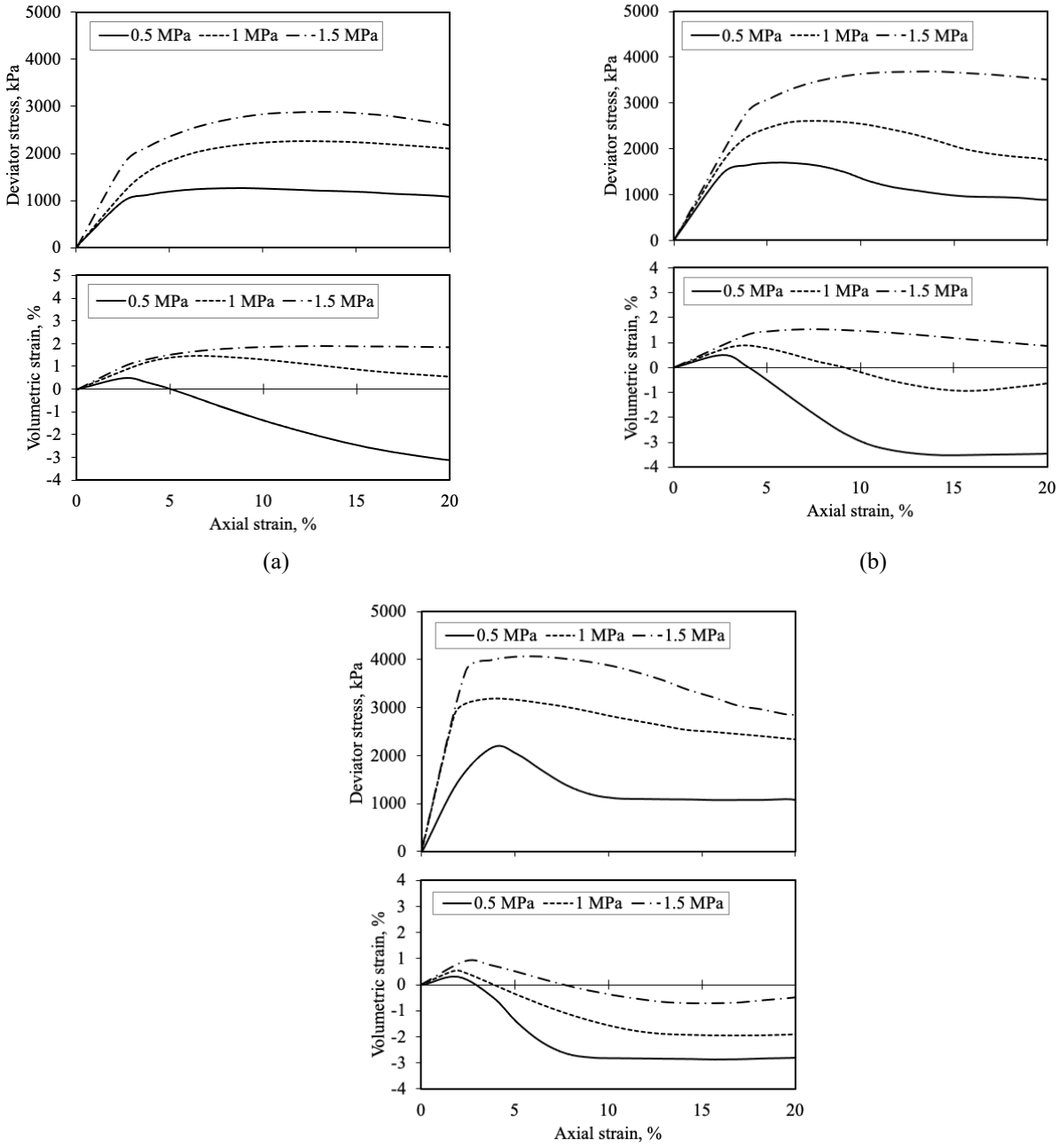

Fig. 5 Stress-strain relationship and volume change behavior of the CSA-treated sand sample: (a) 3%, (b) 5% and (c) 7%, for 14 days curing

increases the peak deviator stresses, while the axial strain is decreased to the peak and increases dilatation during shearing. Therefore, as the CSA cement content increases, the stress-stress behavior of the treated samples shifts from ductility to brittleness.

After the triaxial testing, CSA-treated samples underwent scanning electron microscope (SEM) analysis to assess the material deformation, particle crushing, and cement bond breaking caused by shearing. Figs. 6 and 7 show typical photomicrographs of samples sheared at various CSA cement contents and confining pressures, respectively.

Fig. 6 shows that the magnitude of particle crushing and bond breakage is relatively large in the loose condition (Fig. 6(a)) and gradually decreases as the relative density increases (Figs. 6(b) and 6(c)). It shows the effect of density on the particle crushing and bond breaking of the CSA-treated samples. Also, Fig. 6 shows that the level of particle breakage in the CSA-treated samples at high confining pressures decreases with decreasing void ratio.

Hence, the amount of particle crushing and bond breakage decreases during shearing with an increase in cement content. On the other hand, it can be observed from Fig. 7 that as the confining pressure increases, the particle

Table 3 Summary of the CD triaxial tests results

Test ID	Initial state			Failure condition				Ultimate condition			
	cc, %	σ'_3, kPa	t, days	q_{peak}, kPa	p'_{peak}, kPa	φ'_{peak}, °	c'_{peak}, kPa	q_{ult}, kPa	p'_{ult}, kPa	φ'_{ult}, °	c'_{ult}, kPa
CD-0/0.5	0	500	-	1006.6	845.3	24.9	7.1	714.1	747.1	23.4	3.6
CD-0/1	0	1000	-	1738.4	1588.7	24.9	7.1	1607.4	1544.6	23.4	3.6
CD-0/1.5	0	1500	-	2174.8	2232.8	24.9	7.1	1871.4	2131.5	23.4	3.6
CD-3/0.5/7	3	500	7	1211.5	913.0	28.9	79.6	906.1	812.2	30.0	4.3
CD-3/1/7	3	1000	7	2104.6	1711.6	28.9	79.6	2052.0	1693.2	30.0	4.3
CD-3/1.5/7	3	1500	7	3087.0	2537.8	28.9	79.6	3038.5	2521.5	30.0	4.3
CD-3/0.5/14	3	500	14	1254.4	928.1	33.6	117.9	1063.3	864.8	26.7	9.3
CD-3/1/14	3	1000	14	2260.6	1762.6	33.6	117.9	1750.2	1593.2	26.7	9.3
CD-3/1.5/14	3	1500	14	2892.9	2474.2	33.6	117.9	2554.6	2361.4	26.7	9.3
CD-5/0.5/7	5	500	7	1580.6	1036.3	29.1	178.6	991.7	839.1	29.1	18.6
CD-5/1/7	5	1000	7	2424.3	1817.9	29.1	178.6	1916.3	1647.3	29.1	18.6
CD-5/1.5/7	5	1500	7	3483.4	2670.4	29.1	178.6	2894.6	2474.6	29.1	18.6
CD-5/0.5/14	5	500	14	1696.8	1075.8	30.0	194.3	880.8	801.5	28.5	31.4
CD-5/1/14	5	1000	14	2607.5	1879.3	30.0	194.3	1750.2	1593.2	28.5	31.4
CD-5/1.5/14	5	1500	14	3694.7	2740.9	30.0	194.3	3514.3	2680.8	28.5	31.4
CD-7/0.5/7	7	500	7	2152.4	1227.4	28.5	341.4	1065.8	863.7	28.3	42.1
CD-7/1/7	7	1000	7	2975.2	2000.9	28.5	341.4	1921.1	1648.4	28.3	42.1
CD-7/1.5/7	7	1500	7	3863.0	2796.8	28.5	341.4	2870.9	2465.3	28.3	42.1
CD-7/0.5/14	7	500	14	2186.4	1238.6	29.2	358.2	1057.1	861.5	28.2	42.9
CD-7/1/14	7	1000	14	3185.6	2072.9	29.2	358.2	2311.5	1778.6	28.2	42.9
CD-7/1.5/14	7	1500	14	4079.8	2869.8	29.2	358.2	2851.9	2459.8	28.2	42.9

Note: CD-A/B/C: "CD" is consolidated drained triaxial test. "A" is cement content, "B" is confining pressure in MPa and "C" is number of curing days

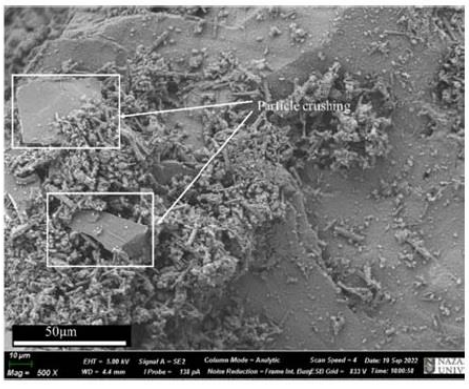

(a)

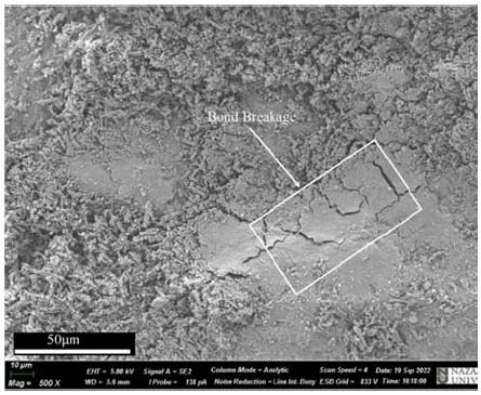

(b)

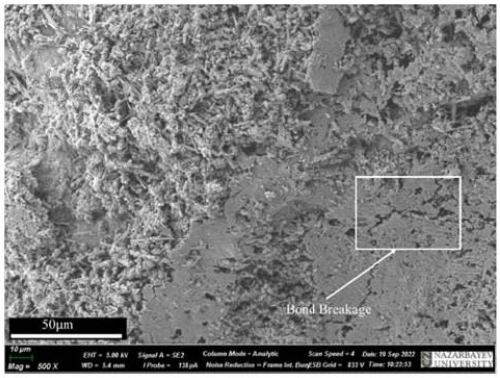

(c)

Fig. 6 SEM photographs of cemented sand samples (a) 3% (b) 5% (c) 7% after shearing at 1 MPa confining pressure

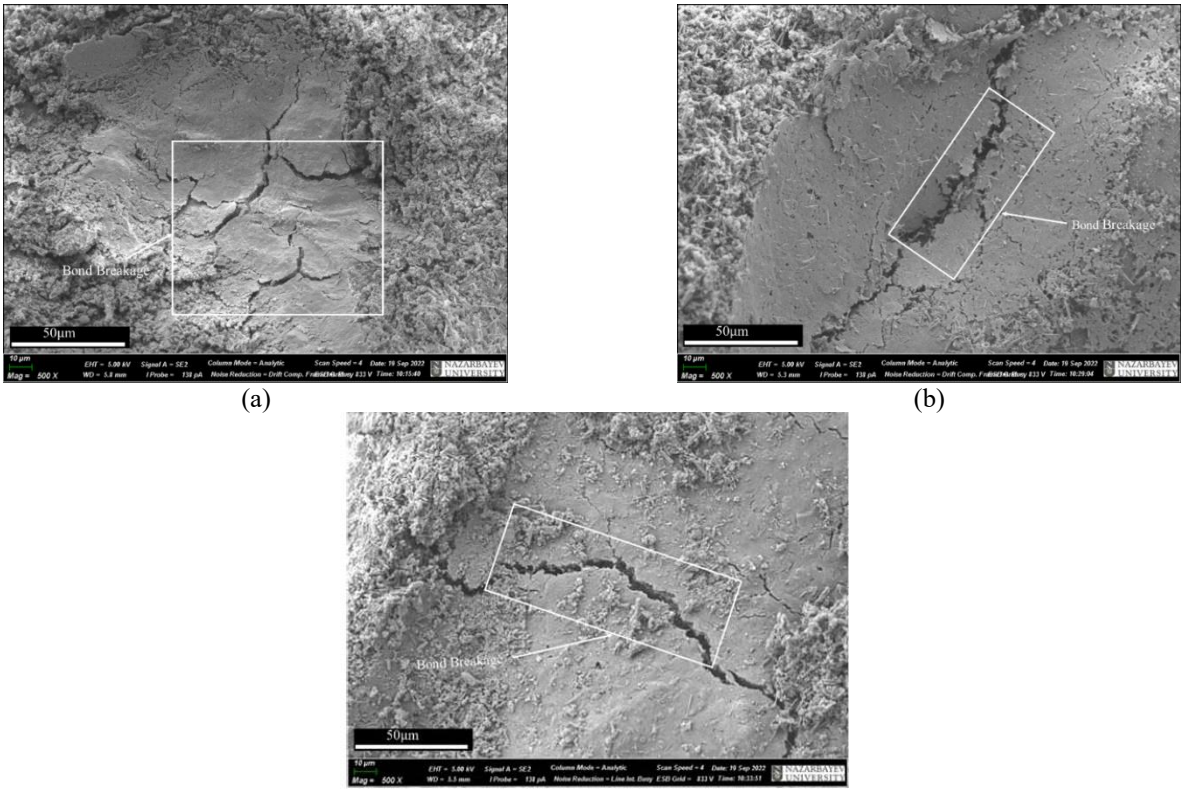

(a) (b) (c)

Fig. 7 SEM photographs of samples with 7% cement content after shearing (a) 0.5 MPa, (b) 1.0 MPa and (c) 1.5 MPa

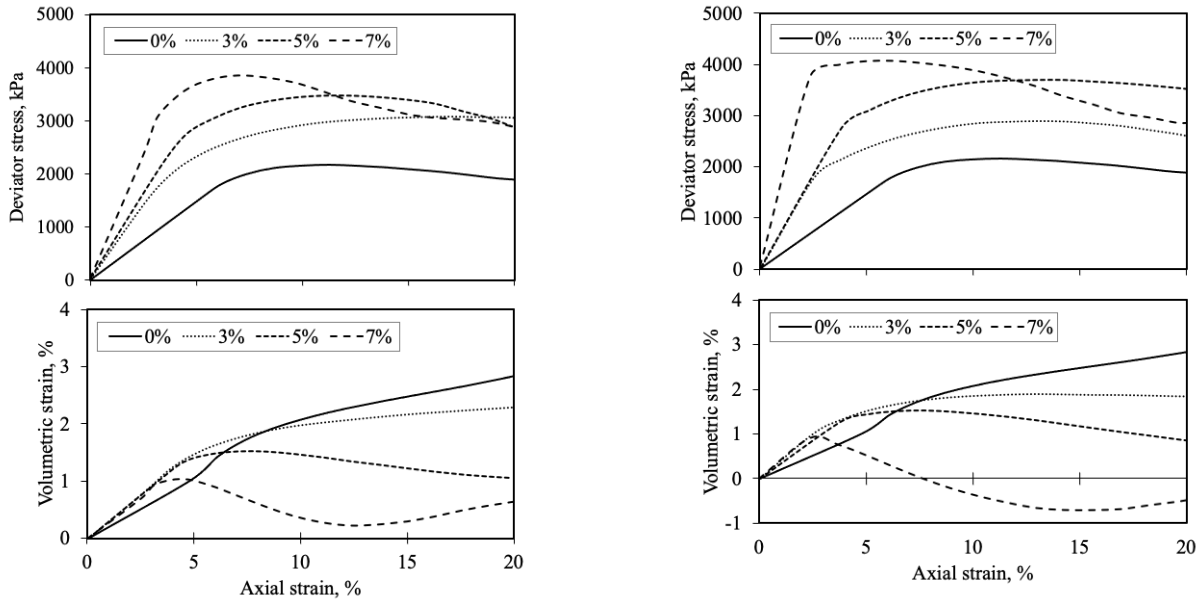

(a) (b)

Fig. 8 Stress-strain relationship and volume change behavior of the CSA-treated sand sample for σ3' = 1.5 MPa at the curing periods of (a) 7 days and (b)14 days

crushing and bond damage of the CSA-treated samples increases. This finding is consistent with the previous experimental research on cemented sand (e.g Marri *et al.* 2012, Schnaid *et al.* 2001).

4. Discussion

4.1 Stress-strain behavior

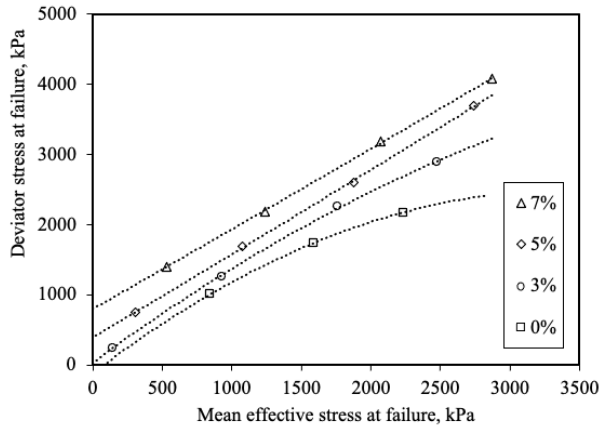

Fig. 9 Failure envelopes of CSA cemented and uncemented sand

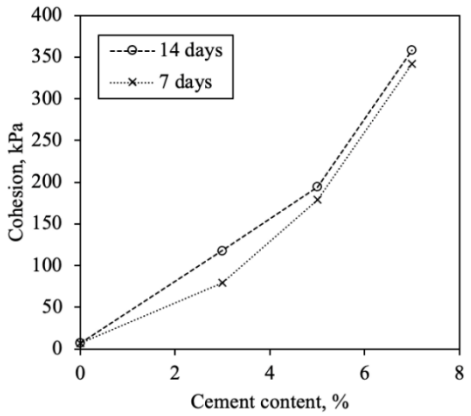

Fig. 10 Effect of CSA cement content on cohesion intercept

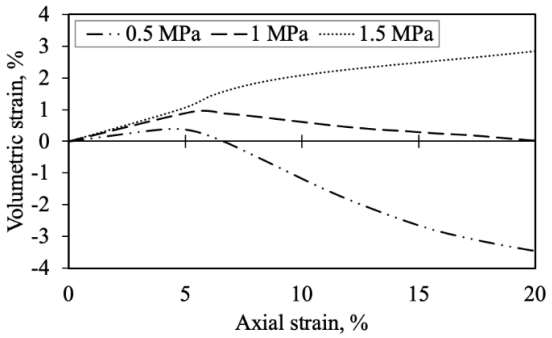

Fig. 11 Suppression of the dilatancy by increasing confining pressure for untreated sand

The stress-strain behavior of sand is influenced by the addition of CSA cement, as illustrated in Figs. 4 and 5 from the previous section. To better explain the effect of cement on the stress-strain and volumetric strain relationship of the sand, three results of tests carried out at various cement contents at the same effective confining stress σ_3' = 1.5 MPa are compared in Fig. 8.

The tests conducted at the same confining pressure of 1.5 MPa were used to explain further the effect of confining pressure on the treated samples because it is the maximum confining pressure employed in this study. Understanding soil behavior at high pressure would be beneficial to comprehend better settings like deep pile foundations and tunnels, among others.

Fig. 8 shows that, as the degree of cementation increases, the axial strain at failure for the tested sample also decreases. Furthermore, the initial stiffness and peak deviator stress of the treated sand samples increase as CSA cement content increases. For instance, the peakdeviator stress at σ'_3 = 1.5 MPa increased from 3,477 kPa to 3,856 kPa (11% increase) when CSA cement content increased from 5% to 7%.

The volumetric strain curves of the tests carried out onthe CSA-treated sand samples at 1.5 MPa confining pressure are also compared in Fig. 8. From Fig. 8(a), it can be observed that all of the samples exhibited compression. However, all samples exhibited compression in Fig. 8(b) except for 7%, which had an initial compression followed by a slow dilation. Hence, as the cement content increase, there is a reduction in the compression behavior of the sand at high confining pressure. Also, with the addition of various CSA cement content to the uncemented sand, there was an increase in the initial stiffness, peak deviator stress, and a decrease in the axial strain at failure. Similarly, the stress-strain behavior of the samples changes from ductility to brittleness as the CSA cement increases. Furthermore, with an increase in the confining pressure, there was an increase in the peak deviator stress and amount of compression during shearing. Hence, the stress-strain and volumetric strain behavior of the CSA cement-treated sample was greatly influenced by the degree of cementation and high confining pressure (e.g., Clough *et al.* 1981, Lee1a *et al*. 2019, Marri *et al.* 2012, Schnaid *et al*. 2001, Ud-din *et al.* 2011).

4.2 Failure characteristics

Because of its cohesive-frictional nature, the friction angle and cohesion intercept significantly alter the failure behavior of CSA-treated sand samples. In addition, all of the tests done in this study were conducted under drained conditions. Hence, the peak state achieved from each test reflects the failure condition of the treated sand samples.

Fig. 9 shows the failure states obtained from all the tests conducted in this study on the deviator stress at the failure-mean effective stress plane. The failure data from tests with cement contents of 0%, 3%, 5%, and 7% were used to generate the best-fitting failure envelopes. Additionally, the failure envelopes were extrapolated to zero confinement. Fig. 9 shows that the failure envelopes are curved. However, there is an increase in the curvature of the failure envelopes as cement content increases. Meanwhile, several researchers have reported curved envelopes for cemented soils and almost linear for uncemented sandy gravel material (Asghari *et al*. 2003, Haeri *et al*. 2005, Marri *et al*. 2012, Ud-din *et al*. 2011).

Moreover, Fig. 9 illustrates that with the increase in CSA cement content, there is an increase in the curvature of the failure envelope. The failure envelopes move to higher stress with increasing CSA cement content, indicating that

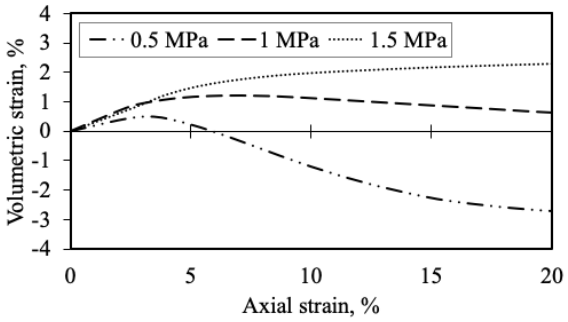

(a)

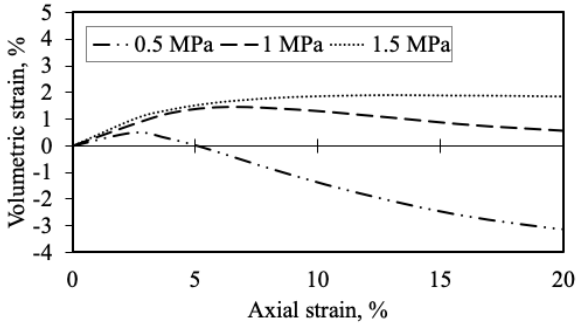

(b)

Fig. 12 Suppression of the dilatancy by increasing confining pressure for CSA-treated sand samples with 3% cement content at (a) 7 days curing and (b) 14 days curing

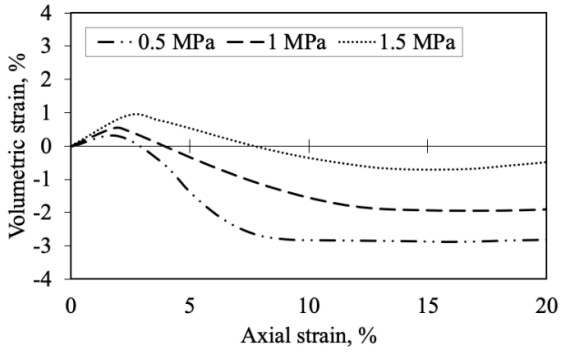

Fig. 13 Suppression of the dilatancy by increasing confining pressure for CSA-treated sand samples with 7% cement content at (a) 7 days curing and (b) 14 days curing

cohesion intercept and intercept particle cohesion of the sand increases with CSA cement content (Fig. 9). It also indicates that the slope of the failure envelopes changes from a linear to a non-linear curve as the CSA cement content decreases. It could result from the particle and bond breakage during the shearing of the treated samples at high confining pressure. Consequently, the effect of cementation on treated sand samples is significantly more significant at low confining pressures than at high confining pressures. However, the observation would be verified with higher confining pressures in the future study compared to confining pressures used in this study.

Considering the cohesive-frictional characteristics of the sand samples treated with CSA, the shear strength may be described as a function of the friction angle and the cohesion intercept. Fig. 10 illustrates the relationship between the cement content and cohesion intercept. The frictional angle and cohesion intercepts were obtained by plotting the mohr-coulomb diagram for all tests with different cement contents sheared and at different confining pressures ranging from 0.5 to 1.5 MPa. It can also be observed from Fig. 10 that as the cement content increase, the cohesion between the particles of treated samples also increases. The friction angle and cohesion intercept

obtained from the mohr-coulomb diagrams are shown in Table 3.

4.3 Stress-dilatancy relationship

Whenever a dense sand sample is sheared in a triaxial test, there is an increase in volume, often referred to as dilation. It is due to the geometrical constraints placed by the fabric against applied stresses during shearing. Nevertheless, as shown in Figs. 11 to 13, at higher confining pressures, the volumetric behavior of sandy material is often suppressed during shearing. Hence, the dilatancy of the CSA-treated sample can be influenced by the presence of CSA cement, which increase the cohesion or bonding between the particles of treated sand.

Also, it can be observed from the Figures that an increase in confining pressure suppresses the amount of dilation in the volumetric strain curve of the tested samples. Samples sheared under 1 MPa all exhibited an initial compression behavior followed by subsequent dilation. The volumetric strain of sand, as shown in Figs. 11 and 12, agrees well with the experimental results published in the literature (Marri *et al.* 2012, Ud-din *et al.* 2011).

5. Conclusions

This study investigated the effect of CSA cement content on its shear strength and mechanical behavior by conducting consolidated drained (CD) triaxial tests with high confining pressures. The effect of both CSA cement content and confining pressure on the stress-strain and volumetric behavior during shearing and failure characteristics were discussed. The following conclusions were drawn based on the results of the tests:

1. The CSA cement content and confining pressure significantly influence the stress-strain and volumetric behavior of the CSA-treated sand samples. As the CSA cement content increases, the peak deviatoric stress increases, although it reduces the amount of compression during shearing. However, with an increase in confining pressure, there is an increase in the peak deviator stress and amount of compression during shearing. Hence, the q-ε_a behavior of the treated samples becomes ductile with an increase in confining pressure. But brittle with an increase in CSA cement content.
2. The CSA cement content and the confining pressure

also impact the failure characteristic of the sand. With an increase in the CSA cement content, the failure envelopes move to higher stress, indicating that the cohesion intercept of the sand will increase. Also, with an increase in confining pressure, the slope of the failure envelopes reduces, meaning that confining pressure influences the curvature of the failure envelopes. Hence at high confining pressure, the shear strength of the CSA-treated sample decrease.

3. The CSA cement content and the confining pressure also affect the stress-dilatancy of the CSA-treated sand samples. With the addition of CSA cement content, there is an increase in cohesion and bonding between the sand particle at specific confining pressures. Hence, the peak deviatoric stress increases with an increase in the CSA cement content. The increase in confining pressure reduces the amount of dilation at specific CSA cement content.
4. The scanning electron microscopy (SEM) analysis revealed that shearing causes the crushing of the sand particles and the rupture of the cement bond. Consequently, the degree of sand particle breaking during shearing increases as confining pressure increases and decreases as CSA cement content increases.

Acknowledgments

This research was funded by the Nazarbayev University, Collaborative Research Project (CRP) Grant No. 11022021CRP1508 and Faculty Development Competitive Research Grant Program (FDCRGP) Grant No. 20122022FD4115. Any opinions, findings, conclusions, or recommendations expressed in this material are those of the author(s) and do not necessarily reflect the views of Nazarbayev University.

References

Airey, D. (1993), "Triaxial testing of naturally cemented carbonate soil", *J. Geotech. Eng.*, **119**(9), 1379-1398. https://doi.org/10.1061/(ASCE)0733-9410(1993)119:9(1379).

Amini, Y. and Hamidi, A. (2014), "Triaxial shear behavior of a cement-treated sand–gravel mixture", *J. Rock Mech. Geotech. Eng.*, **6**(5), 455-465. https://doi.org/10.1016/j.jrmge.2014.07.006.

Armaghani, D.J., Mirzaei, F., Shariati, M., Trung, N.T., Shariati, M. and Trnavac, D. (2020), "Hybrid ANN-based techniques in predicting cohesion of sandy-soil combined with fiber", *Geomech. Eng.*, **20**(3), 191-205. https://doi.org/10.12989/gae.2020.20.3.191.

Asghari, E., Toll, D. and Haeri, S. (2003), "Triaxial behaviour of a cemented gravely sand, Tehran alluvium", *Geotech. Geol. Eng.*, **21**(1), 1-28. https://doi.org/10.1023/A:1022934624666.

Assel, J., Sagidullina, N., Kim, J. and Moon, S.W. (2020), "Effect of cyclic freezing-thawing on strength and durability of sand stabilized with CSA cement", *Proceedings of the 2020 World Congress on Advances in Civil, Environmental, & Materials Research*,

ASTM/D698 (2012), Standard test methods for laboratory compaction characteristics of soil using standard effort, *ASTM D698*. https://doi.org/10.1520/D0698-12R21

ASTM/D7181-20 (2015), *Standard Test Method for Consolidated Drained Triaxial Compression Test for Soils*. ASTM International. https://doi.org/10.1520/D7181-20

Bazarbekova, A., Shon, C.S., Kissambinova, A., Kim, J.R., Zhang, D. and Moon, S.W. (2021), "Potential of limestone powder to improve the stabilization of sulfate-contained saline soil", *Proceedings of the IOP Conference Series: Materials Science and Engineering*.

Bisserik, A., Kim, J., Satyanaga, A. and Moon, S.W. (2021), "Characterization of CSA cemented-treated sands via discrete element method", *Proceedings of the AIP Conference Proceedings*.

Chang, I. and Cho, G.C. (2014), "Geotechnical behavior of a beta-1, 3/1, 6-glucan biopolymer-treated residual soil", *Geomech. Eng.*, **7**(6), 633-647. https://doi.org/10.12989/gae.2014.7.6.633.

Chang, I., Im, J. and Cho, G.C. (2016), "Geotechnical engineering behaviors of gellan gum biopolymer treated sand", *Can. Geotech. J.*, **53**(10), 1658-1670. https://doi.org/10.1139/cgj-2015-0475.

Clough, G.W., Sitar, N., Bachus, R.C. and Rad, N.S. (1981), "Cemented sands under static loading", *J. Geotech. Eng. Division*, **107**(6), 799-817. https://doi.org/10.1061/AJGEB6.0001152.

Consoli, N., Schnaid, F., Prietto, P. and Rohlfes, Jr. J. (1996), "Engineering properties of residual soil-cement mixtures", *Proceedings of the 2nd Int. Conf. on Ground Improvement Geosystems: Grouting and Deep Mixing*.

Ding, M., Zhang, F., Ling, X. and Lin, B. (2018), "Effects of freeze-thaw cycles on mechanical properties of polypropylene Fiber and cement stabilized clay", *Cold Reg. Sci. Technol.*, **154**, 155-165. https://doi.org/10.1016/j.coldregions.2018.07.004.

Gartner, E. (2004), "Industrially interesting approaches to "low-CO2" cements", *Cement Concrete Res.*, **34**(9), 1489-1498. https://doi.org/10.1016/j.cemconres.2004.01.021.

Ghiyas, S.M.R. and Bagheripour, M.H. (2020), "Stabilization of oily contaminated clay soils using new materials: Micro and macro structural investigation", *Geomech. Eng.*, **20**(3), 207-220. https://doi.org/10.12989/gae.2020.20.3.207.

Haeri, S.M., Hamidi, A. and Tabatabaee, N. (2005), "The effect of gypsum cementation on the mechanical behavior of gravely sands", *Geotech. Test. J.*, **28**(4), 380-390. https://doi.org/10.1520/GTJ12574

Juenger, M., Winnefeld, F., Provis, J.L. and Ideker, J. (2011), "Advances in alternative cementitious binders", *Cement Concrete Res.*, **41**(12), 1232-1243. https://doi.org/10.1016/j.cemconres.2010.11.012.

Jumassultan, A., Sagidullina, N., Kim, J., Ku, T. and Moon, S.W. (2021), "Performance of cement-stabilized sand subjected to freeze-thaw cycles", *Geomech. Eng.*, **25**(1), 41-48. https://doi.org/10.12989/gae.2021.25.1.041.

Kazmi, Z.A. (2020), "Improvement in shear strength characteristics of desert sand using shredded plastic waste", *Geomech. Eng.*, **20**(6), 497-503. https://doi.org/10.12989/gae.2020.20.6.497.

Lee1a, S., Im, J., Cho, G. and Chang, I. (2019), "Laboratory triaxial test behavior of xanthan gum biopolymer-treated sands", *Geomech. Eng.*, **17**(5), 445-452. https://doi.org/10.12989/gae.2019.17.5.445.

Mahedi, M., Cetin, B. and White, D.J. (2020), Cement, lime, and fly ashes in stabilizing expansive soils: performance evaluation and comparison", *J. Mater. Civil Eng.*, **32**(7), 04020177. https://doi.org/10.1061/(ASCE)MT.1943-5533.0003260.

Marri, A., Wanatowski, D. and Yu, H. (2012), "Drained behaviour of cemented sand in high pressure triaxial compression tests", *Geomech. Geoeng.*, **7**(3), 159-174. https://doi.org/10.1080/17486025.2012.663938.

Moon, S.-W., Vinoth, G., Subramanian, S., Kim, J. and Ku, T.

(2020), "Effect of fine particles on strength and stiffness of cement treated sand", *Granular Matter.*, **22**(1), 1-13. https://doi.org/10.1007/s10035-019-0975-6.

Pooni, J., Robert, D., Giustozzi, F., Setunge, S., Xie, Y. and Xia, J. (2020), "Novel use of calcium sulfoaluminate (CSA) cement for treating problematic soils", *Constr. Build. Mater.*, **260**, 120433. https://doi.org/10.1016/j.conbuildmat.2020.120433.

Sagidullina, N., Abdialim, S., Kim, J., Satyanaga, A. and Moon, S.W. (2022a), "Influence of freeze–thaw cycles on physical and mechanical properties of cement-treated silty sand", *Sustainability*, **14**(12), 7000. https://doi.org/10.3390/su14127000.

Sagidullina, N., Abdialim, S., Kim, J., Satyanaga, A. and Moon, S.W. (2022b), "Stabilization of silty sand with CSA cement under freeze-thaw cycles", *Proceeding of the 10th International Conference on Physical Modelling in Geotechnics (ICPMG)*.

Sargent, P., Hughes, P. and Rouainia, M. (2016), "A new low carbon cementitious binder for stabilising weak ground conditions through deep soil mixing", *Soils Found.*, **56**(6), 1021-1034.

Schnaid, F., Prietto, P.D. and Consoli, N.C. (2001), "Characterization of cemented sand in triaxial compression", *J. Geotech. Geoenviron. Eng.*, **127**(10), 857-868. https://doi.org/10.1061/(ASCE)1090-0241(2001)127:10(857).

Schneider, M., Romer, M., Tschudin, M. and Bolio, H. (2011), "Sustainable cement production—present and future", *Cement Concrete Res.*, **41**(7), 642-650. https://doi.org/10.1016/j.cemconres.2011.03.019.

Singh, R., Ray, D., Mehrotra, A. and Afaque Khan, M. (2018), "A review paper on comparative study of soil stabilization with widely used admixtures like lime, cement, flyash and bitumen emulsion", *Int. J. Eng. Trends Technol.*, **58**(2), 96-99. https://doi.org/10.14445/22315381/IJETT-V58P218.

Subramanian, S., Khan, Q. and Ku, T. (2019), "Strength development and prediction of calcium sulfoaluminate treated sand with optimized gypsum for replacing OPC in ground improvement", *Constr. Build. Mater.*, **202**, 308-318. https://doi.org/10.1016/j.conbuildmat.2018.12.121.

Subramanian, S., Moon, S.W., Moon, J. and Ku, T. (2018), "CSA-treated sand for geotechnical application: microstructure analysis and rapid strength development", *J. Mater. Civil Eng.*, **30**(12), 04018313. https://doi.org/10.1061/(ASCE)MT.1943-5533.0002523.

Ud-din, S., Marri, A. and Wanatowski, D. (2011), "Effect of high confining pressure on the behaviour of fibre reinforced sand", *Geotech. Eng. J. SEAGS & AGSSEA*, **42**(4), 69-76.

Ukrainczyk, N., Franković Mihelj, N. and Šipušić, J. (2013), "Calcium sulfoaluminate eco-cement from industrial waste", *Chem. Biochem. Eng. Q.*, **27**(1), 83-93.

Vinoth, G., Moon, S.W., Kim, J. and Ku, T. (2018), "Effect of fine particles on cement treated sand", *Proceedings of China-Europe Conference on Geotechnical Engineering*.